

# A Fuel-Cell Based Boost Converter Model Using Euler-Lagrange Equation

Atila Eskandarnezgad<sup>\*1</sup>

**Abstract** – This paper presents a new modeling technique for fuel cell based switching converters. Often a step-up converter is used in the fuel cell applications due to its relative low voltage. Here a boost converter is used to convert the fuel cell voltage to the desired load level. The aim of this paper is to study through analysis and simulation, the voltage mode control and dynamic modeling of series interconnected topology of a fuel cell based system. Euler-Lagrange (EL) equation is used here as a modeling technique which relies on the energy balance equilibrium because fuel cell based systems can be considered as an energy processing structure. The fuel cell must be protected against the current harmonics or sudden transients so that it provides the regulated voltage for output load. We use a LC filter between fuel cell and converter to prevent the current harmonics from reaching the fuel cell since this may lead to oxygen starvation phenomena around the electrodes surface or other faults. The proposed modelling procedure is applicable for any other converter based on fuel cells. Finally, simulation is done by PSIM and MATLAB softwares to validate the proposed modeling technique. We run both the frequency and time domain analysis to show that the proposed modeling technique coincides exactly with the simulation results.

**Keywords:** Fuel Cell, Boost Converter, Dynamic Modeling, Euler-Lagrange Equation.

## I. Introduction

Due to the increased demand of electrical energy, it has become more important to produce energy in an ecologically friendly manner. Besides, fossil fuels are limited; this leads to higher prices for the energy. In future, then the main part of our energy demand has to be responded from renewable energy sources such as hydro, photovoltaic or wind power [1]. One main disadvantage of the above mentioned sources is their non-continuous energy production. For example, there are some lazy times when the sun does not shine or the wind does not blow [2]. One method to solve this problem is the generation of hydrogen by electrolysis in low-load times. Then, this hydrogen could be used as energy storage to support the renewable energy sources in the idle times or to deliver energy when the photovoltaic and wind farms do not work. This can be done using fuel cells which have relatively good efficiency, clean emission and operation with pure hydrogen [3]. This feature makes fuel cell an attractive choice for mobile applications. A typical fuel cell setup and its operation principle are

shown in Fig. 1a.

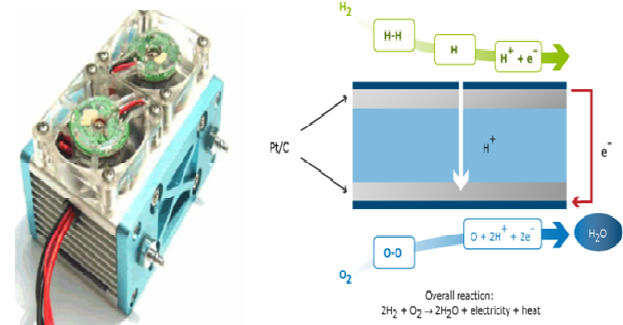


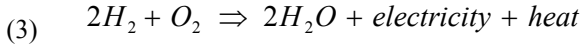
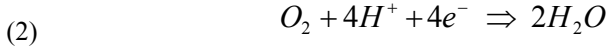
**Fig. 1a** Typical fuel cell setup (left) and its operation principle (right)

The chemical principle of fuel cells was first discovered in 1839 by William Grove, a British physicist. It consists of an electrolyte sandwich between two electrodes. The electrolyte has a special property: it passes positive ions through while blocks the electrons. Hydrogen gas moves from one electrode (called anode) whereof, with the help of a catalyst, it separates into electrons and hydrogen protons. Protons move to other electrode (called cathode) by the electrolyte path while the electrons flow through the external circuit where they create electricity. Simple fuel cell overall reaction can be represented by the following equations [4].



<sup>1\*</sup> **Corresponding Author** : Department of Electrical Engineering, Iran University of Technology(IUST), Tehran, Iran, Email: a.skandamezhad@yahoo.com

Received 2017.10.25 ; Accepted 2018.12.15



The net voltage of a cell is between 0-1 V depending on its load and operating condition. The typical value of the fuel cell voltage is about 0.7 V; thus, to obtain higher voltages, several cells must be connected serially. Fuel cells have several advantages when used in combustion engines and batteries. The combustion engines first convert the fuel energy to thermal energy and then convert the thermal energy to mechanical energy; furthermore its efficiency is rather low in comparison with fuel cells, where the fuel energy is directly converted to the electricity [3]. If hydrogen is used as fuel, the outcome of reaction is water and heat; thus they are considered as a zero emission power generator and do not create any pollutant. Also, batteries convert the chemical energy directly to electricity, but their reactant is stored internally and must be replaced or recharged when they are exhausted. Fuel cell reactant is stored internally and its inputs (oxygen and hydrogen) are feed by free air or high pressure tanks. The tanks need rather little time to be charged compared to batteries. Here, we employed a boost converter with voltage mode control to convert the cell voltage to desired level and used EL equation for modeling and regulating the loop properties. The presented model is new and subtle and can be used for other converter kinds.

## II. Electrical Model of a Fuel Cell

Among the fuel cells family, the proton exchange membrane (PEM) fuel cells are mostly used in low power and portable applications because of their high efficiency and low operating temperature [4]. Fig. 1b shows the fuel cell polarization curve or voltage-current relation and its circuit model which are applicable to calculate the cell impedance at a given operating point.

Reversible open circuit voltage (EOC) of an H-30 fuel cell can be calculated using the following,

$$E_{OC} = \frac{-\Delta g_f}{z.F} \quad (4)$$

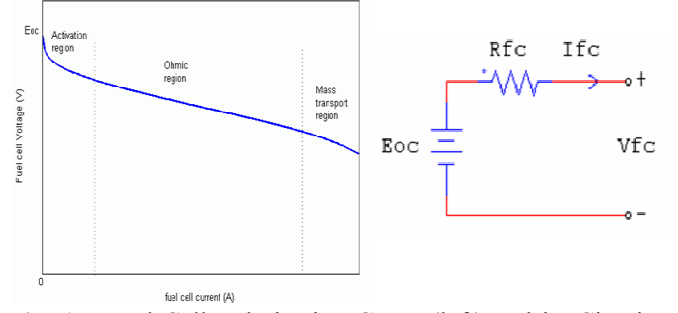


**Fig. 1b.** Fuel Cell Polarization Curve (left) and its Circuit Model (right)

in which  $\Delta g_f$  is the difference between Gibbs free energy of the product and reactant,  $F$  is the faraday constant equal to 96485 Farads and  $z$  is electron transfer ratio per mole ( $z$  is equal to 2 for PEM H-30 fuel cell). The Gibbs free energy defines the available energy to do external work and varies by pressure and temperature. Negative value of Gibbs ratio means that the energy releases from the cell [5].

As seen in Fig. 1b, open circuit initial voltage is lower a little than  $E_{oc}$ . First there is a rapid initial fall in voltage, then the voltage falls more linearly and less rapidly; and then by increasing the current it falls again rapidly. Voltage drop phenomenon of a fuel cell occurs due to four major causes: I) Activation loss, II) Fuel crossover or internal current effect, III) Ohmic loss, IV) Mass transport or concentration loss. By considering the losses effect already described, one can present a formula for polarization curve as:

$$V = E_{OC} - A \ln(i) - r.i + m \exp(ni) \quad (5)$$

This equation, however, does not work at very low current and we advise to use it in currents above 1 mA/cm<sup>2</sup>. In (5)  $E_{oc}$  term can be calculated using (4),  $A$  symbol is Tafel equation constant;  $r$  is area specific resistance of the electrolyte,  $m$  and  $n$  are constants in the mass-transfer over voltage equation. Depending on the working region of a cell, it is possible to neglect appropriate small terms in (5).

## III. Boost Converter Modeling Using Euler-Lagrange Equation

Euler-Lagrange (EL) equation is used for deriving a physically motivated model of the dc to dc switching converter of a Boost type circuit. The EL equation was developed in 1750's by Euler and Lagrange in connection with their studies of a mechanical problem [6]. In EL mechanics, the evolution of a physical system is described by solutions to the EL equation activity of the system.

Comparing with Newton's mechanic, this method has the same form in any generalized coordination [7]. The non-conservative EL dynamics of a circuit can be classically characterized as in the following [8].

$$\frac{d}{dt} \left( \frac{\partial \ell(q, \dot{q})}{\partial \dot{q}} \right) - \frac{\partial \ell(q, \dot{q})}{\partial q} = - \frac{\partial \psi(\dot{q})}{\partial \dot{q}} + \chi(q) \lambda + F_q \quad (6)$$

$$\ell(q, \dot{q}) = \tau(q, \dot{q}) - \nu(q, \dot{q}) \quad , \quad \chi(q) \dot{q}^T = 0 \quad (7)$$

where  $q$ . is the vector of electric current and  $q$  represents its time integral or electric charge. The scalar function  $\ell$  is the Lagrange operator of the system; that is the difference between the kinetic energy (denoted by  $\tau$ ) and potential energy (denoted by  $\nu$ ) of this system. The symbol  $\psi$  is the Raleigh dissipation function of the system and the vector  $F_q$  represents the forcing function associated with each state variable coordinate. The symbol  $\lambda$  is the intermediate artificial variable and  $\chi$  introduces the constraint forces matrix, normally defined by Kirchoff's current law. The circuit components is supposed to have parasitic elements such as transistor leading resistor ( $r_T$ ), diode forward voltage and resistor ( $V_D$ ,  $r_D$ ) and equivalent series resistance (ESR) of inductor ( $r_L$ ) and capacitor ( $r_C$ ). In the proceeding discussions,  $s(t)$  symbol states the transistor position function and can be specified as:

$$s(t) = \begin{cases} 1, & \text{for } t_k \leq t \leq t_k + D_k \cdot T \\ 0, & \text{for } t_k + D_k \cdot T \leq t \leq t_k + T \end{cases} ; t_{k+1} = t_k + T ; k = 0, 1, 2, \dots \quad (8)$$

First, suppose that the transistor is on or  $S(t)=1$ ; in this case, the EL quantities can be readily found as:

$$\tau_1(q, \dot{q}) = \frac{1}{2} L_i \dot{q}_L^2 ; \nu_1(q, \dot{q}) = \frac{1}{2} \frac{q_C^2}{C_o} \quad (9)$$

$$\ell_1(q, \dot{q}) = \tau_1(q, \dot{q}) - \nu_1(q, \dot{q}) = \frac{1}{2} L_i \dot{q}_L^2 - \frac{1}{2} \frac{q_C^2}{C_o} \quad (10)$$

$$\psi_1(q) = \frac{1}{2} R_{out} \dot{q}_C^2 + \frac{1}{2} r_C \dot{q}_C^2 + \frac{1}{2} (r_L + r_T) \dot{q}_L^2 \quad (11)$$

$$F_{qL}^1 = V_{in} ; F_{qC}^1 = 0 \quad (12)$$

where  $F_{qL}$  and  $F_{qC}$  are the generalized forcing functions related to the  $q_L$  and  $q_C$  coordinates, respectively. Now consider the case  $S(t)=0$  as follows:

$$\tau_0(q, \dot{q}) = \frac{1}{2} L_i \dot{q}_L^2 ; \nu_0(q, \dot{q}) = \frac{1}{2} \frac{q_C^2}{C_o} \quad (13)$$

$$\ell_0(q, \dot{q}) = \tau_0(q, \dot{q}) - \nu_0(q, \dot{q}) = \frac{1}{2} L_i \dot{q}_L^2 - \frac{1}{2} \frac{q_C^2}{C_o} \quad (14)$$

$$\psi_0(q) = \frac{1}{2} R_{out} (\dot{q}_L - \dot{q}_C)^2 + \frac{1}{2} r_C \dot{q}_C^2 + \frac{1}{2} (r_L + r_D) \dot{q}_L^2 \quad (15)$$

$$F_{qL}^0 = V_{in} - V_D ; F_{qC}^0 = 0 \quad (16)$$

where  $\tau_0$ ,  $\nu_0$  and  $\psi_0$  are the kinetic, potential and Raleigh dissipation functions of the circuit, respectively. As it can be seen, the dissipation structure of system is only affected by switch position  $S(t)$ . Thus, one can change the EL equation to the universal form as follows:

$$\tau_s(q, \dot{q}) = \frac{1}{2} L_i \dot{q}_L^2 ; \nu_s(q, \dot{q}) = \frac{1}{2} \frac{q_C^2}{C_o} \quad (17)$$

$$\ell_s(q, \dot{q}) = \tau_s(q, \dot{q}) - \nu_s(q, \dot{q}) = \frac{1}{2} L_i \dot{q}_L^2 - \frac{1}{2} \frac{q_C^2}{C_o} \quad (18)$$

$$\psi_s(q) = \frac{1}{2} R_{out} ((1-D)\dot{q}_L - \dot{q}_C)^2 + \frac{1}{2} r_L \dot{q}_L^2 + \frac{1}{2} r_C \dot{q}_C^2 + \frac{1}{2} (D r_T + (1-D) r_D) \dot{q}_L^2 \quad (19)$$

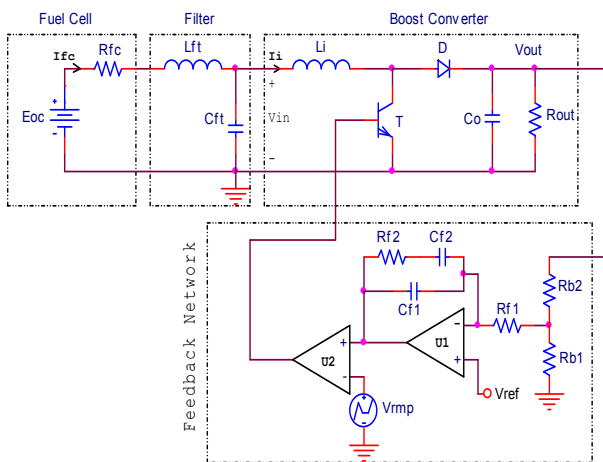


Fig. 2a Entire converter circuitry

There are two state variables in the studied circuit: input inductor current ( $I_L$ ) and output capacitor voltage ( $V_C$ ). The system kinetic and potential energies correspond to the magnetic and electric energies of the circuit, respectively.

$$(20) \quad F_{q_L}^s = V_{in} - (1-D)V_D ; \quad F_{q_C}^s = 0$$

Now, by applying (6) and (7) on (17)-(20), we can rewrite: (21)

$$\begin{cases} L_i \dot{q}_L = -(1-D)\left(\frac{q_C}{C_o} + r_C \dot{q}_C\right) - (r_L + D r_T + (1-D)r_D) \dot{q}_L + (V_{in} - (1-D)V_D) \\ (R_{out} + r_C) \dot{q}_C = R_{out}(1-D) \dot{q}_L - \frac{q_C}{C_o} \end{cases} \quad (22)$$

Using  $x_1=q_L$  and  $x_2=q_C/C_o$  replacements, we can change (21) to (22):

$$\begin{aligned} \dot{X} &= AX + BU \\ \begin{bmatrix} \dot{x}_1 \\ \dot{x}_2 \end{bmatrix} &= \begin{bmatrix} a_{11} & a_{12} \\ a_{21} & a_{22} \end{bmatrix} \begin{bmatrix} x_1 \\ x_2 \end{bmatrix} + \begin{bmatrix} b_{11} & b_{12} \\ b_{21} & b_{22} \end{bmatrix} \begin{bmatrix} u_1 \\ u_2 \end{bmatrix} \\ x_1 &= \dot{q}_L, \quad x_2 = \frac{q_C}{C_o}, \quad u_1 = V_{in}, \quad u_2 = V_D \\ r' &= (R_{out} \parallel r_C), \quad r'' = r_L + D r_T + (1-D)r_D \end{aligned} \quad (23)$$

where state matrix indexes are:

$$\begin{aligned} a_{11} &= \frac{-1}{L_i} ((1-D)^2 r' + r'') ; \quad a_{12} = -\frac{(1-D)}{L_i} \left(1 - \frac{r'}{R_{out}}\right) \\ a_{21} &= \frac{1-D}{C_o} \frac{r'}{r_C} ; \quad a_{22} = -\frac{1}{C_o (R_{out} + r_C)} \\ b_{11} &= 1 ; \quad b_{12} = -(1-D) ; \quad b_{21} = 0 ; \quad b_{22} = 0 \end{aligned} \quad (24)$$

The proposed technique presented here coincides with the classical state space averaging (SSA) method, therefore, it can be used to derive the system transfer function, time response, stability consideration and other control aspects.

$$\begin{cases} \dot{X}(s) = AX(s) + BU(s) \\ Y(s) = CX(s) + DU(s) \end{cases} \Rightarrow \begin{cases} X(s) = (sI - A)^{-1} BU(s) \\ Y(s) = (C(sI - A)^{-1} B + D)U(s) \end{cases} \quad (25)$$

It is necessary to place a low pass filter between the fuel cell and converter input nodes to diminish the current harmonics generated by switching operation. Relative harmonic current of a fuel cell must be reduced down to lower than 3% to avoid it from damaging [9]. The boost converter has also the inherent ability to cancel the current harmonics due to its input inductor.

By supposing the source current and boost current ripples

equal to 2% and 10%, we can use (25)-(28) to calculate the input filter components values:

$$(25) \quad \frac{\Delta I_{fc}}{I_{fc}} = 2\% \quad ; \quad \frac{\Delta I_i}{I_{fc}} = 10\%$$

$$(26) \quad \frac{\Delta I_{fc}}{I_{fc}} = \frac{1}{j\omega C_{ft}} \frac{1}{jL_{ft}\omega + \frac{1}{j\omega C_{ft}} + R_{fc}} \left(\frac{\Delta I_i}{I_{fc}}\right) = 2\%$$

$$(27) \quad \Delta I_i = \frac{V_{out} D (1-D)}{2L_i \cdot f_s}$$

$$(28) \quad L_{ft} = \frac{1}{\omega^2 C_{ft}} \left( -\frac{\Delta I_i}{0.02 I_{fc}} - 1 - \omega R_{fc} C_{ft} \right) \quad ; \quad \omega = 2\pi f_s$$

#### IV. Simulation Results

The closed loop converter consists of feedback circuit, control circuit, pulse width modulator and a power stage block. The input resistance of the closed loop boost converter is negative; this reduces the magnitude of the output impedance by a factor of  $|1+Tcl|$ , where  $Tcl$  is the loop gain. The converter entire circuitry with voltage mode control was shown in fig.2a and the schematic model in fig.2b, where it consists of four blocks: fuel cell block, LC filter, boost converter and feedback network. The feedback network has three parts: resistive divider, compensator ( $T_c$ ) and modulator ( $T_m$ ).

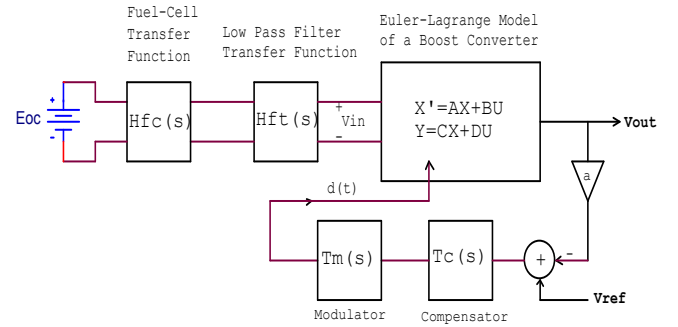


Fig. 2b. Converter averaged model block diagram

Now, we are able to present the simulation results of the proposed converter of fig. 2a and fig. 2b. The Time and frequency domain simulations, (corresponding to, fig. 2a and fig.2b, respectively) have been done within PSIM and MATLAB software packages. The converter parts' values are given in Table 1. First, using (22)-(23), the state matrix and its transfer functions are found; eq.(29) represents the state space averaged equation, (30), the state variables, (31),

resistive dividing ratio, (32), the PI controller function, (33), the modulator ratio, (34), the converter control-to-output transfer function and finally (35), the entire loop gain.

**Table1.** The simulated converter component values

Symbol	Description
Value	
Lft, Cft	Filter inductor and capacitor
20uH, 4.7uF	
Li, rL	Boost inductor and its parasitic
100uH, 0.1Ω	
Co, rc	Boost capacitor and its parasitic
100uF, 0.05Ω	
VD, rD	Diode forward voltage and its resistor
0.5V,0.07Ω	
fs, rT	Transistor resistor and its frequency
100KHz, 0.12Ω	
Rout	Converter output resistor
20Ω	
Rb1, Rb2	Feedback network divider resistors
1KΩ, 19KΩ	
Cf1, Rf1	Feedback network components
150pF, 100KΩ	
Cf2, Rf2	Feedback network components
4.7nF, 100KΩ	
Vref, Vrpm	Reference and ramp voltage
2V, 0-5V:100 KHz	
Vout	Converter output voltage
40V	
U1, U2	Feedback network Op-Amps
LF353	

$$(29) \quad \begin{bmatrix} \dot{X}_1 \\ \dot{X}_2 \end{bmatrix} = \begin{bmatrix} -1120 & -990 \\ +4400 & -1000 \end{bmatrix} \begin{bmatrix} X_1 \\ X_2 \end{bmatrix} + \begin{bmatrix} 1 & -0.2 \\ 0 & 0 \end{bmatrix} \begin{bmatrix} U_1 \\ U_2 \end{bmatrix}$$

(30)

$$X_1 = \dot{q}_L = I_{Li}, \quad X_2 = \frac{q_C}{C} = V_{Co}, \quad U_1 = V_{in}, \quad U_2 = V_D$$

(31)

$$\alpha = \frac{R_{b1}}{R_{b1} + R_{b2}} = 0.05$$

(32)

$$T_c(s) = \frac{1}{R_{f1}C_{f1}} \frac{s + \frac{1}{R_{f2}C_{f2}}}{s(s + \frac{C_{f1} + C_{f2}}{R_{f2}C_{f1}C_{f2}})} = \frac{k_c(s + \omega_{zc})}{s(s + \omega_{pc})}$$

$$k_c = 66.6 \times 10^3, \quad \omega_{zc} = 2.12K(\text{rad/sec}), \quad \omega_{pc} = 68.54K(\text{rad/sec})$$

$$(33) \quad T_m(s) = \frac{1}{V_{rpm}} = 0.2 \approx -14\text{db}$$

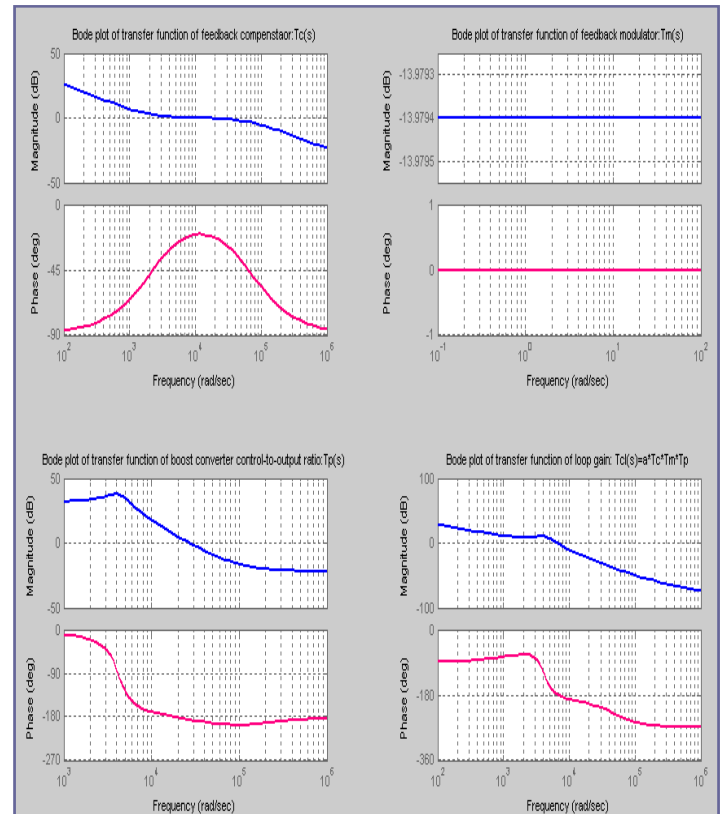
(34)

$$T_p(s) = -\frac{k_p(1 + \frac{s}{\omega_{zp1}})(1 - \frac{s}{\omega_{zp2}})}{1 + \frac{2\zeta s}{\omega_o} + (\frac{s}{\omega_o})^2}; \quad k_p = 38.2$$

$$\omega_o = 4.2K(\text{rad/sec}), \omega_{zp1} = 131K(\text{rad/sec}), \omega_{zp2} = 65.2K(\text{rad/sec})$$

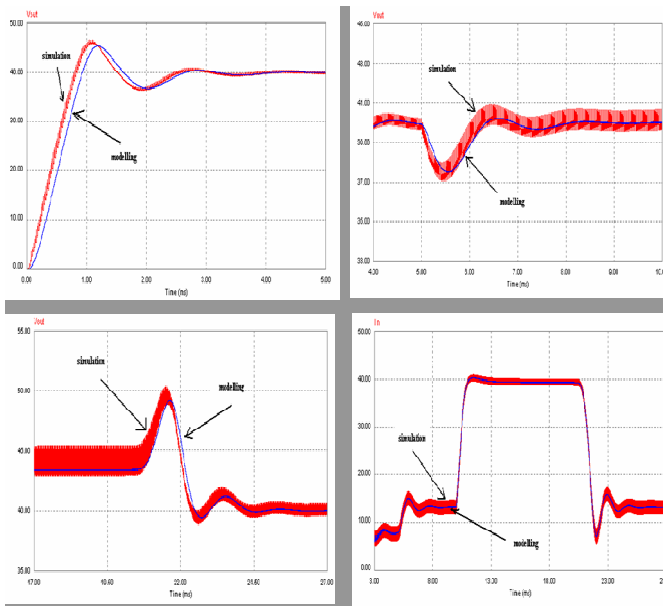
$$(35) \quad T_{cl}(s) = \alpha \times T_c(s) \times T_m(s) \times T_a(s)$$

Fig. 3 shows Bode plots of the system transfer functions using MATLAB, in which the controller function Tc (up-left), the modulator function Tm (up-right), the control-to-output function Tp (down-left) and entire loop gain Tel (down-right) can be seen. The next step is to run the time domain simulation of converter using PSIM where it can be seen in fig. 4; in this figure, the up-left shows the converter output voltage during the system starts up, the up-right, the output voltage when load increases about 50%, the down-left when the reference voltage decreases about 10% and the down-right, the converter input current. All the figures compare results from the simulation with those from the modeling.



**Fig. 3.** Frequency response of the converter transfer

functions ( $T_c$ ,  $T_m$ ,  $T_p$  and  $T_{cl}$ )



**Fig. 4.** Time domain simulation and comparison of the converter output voltage and input current

## V. CONCLUSION

We introduced a new technique for modeling the fuel cell based converter. The converter employed here is a boost type circuit which increases the fuel cell voltage (12V) to a desired level (40V). First, we explained the fuel cell internal effects by means of mathematical equations and expressed its exact model. Then, by describing the Lagrange differential equation, the averaged model of the boost converter was presented. Afterwards, compensation of the converter's output voltage using an integral-single-lead controller was suggested. This was consisted of three main sections: the resistive divider network, the error amplifier and the modulator network. To reduce the current ripples supplied by fuel cell and to protect it, we designed and inserted a LC filter between the fuel cell and boost converter. Finally, to verify and validate the proposed modeling technique, we assumed typical values for the converter components and run simulations of the model within PSIM and MATLAB. The transfer functions of the proposed system blocks were also derived. Simulation results exhibited a stable and fast dynamic response for the designed system. For the future works, it is worthy to do the EL model for other type of dc converters and to compare the current-mode-control response with the voltage-mode-control.

## References

- [1] A. Skandarneshad, A. Rahmati, A. Abrishamifard, "Analysis and control of a unity power factor electrical-vehicle charger using dc clamped SEPIC converter with electro-magnetic compatibility", *Compt. rend. Acad. bulg. Sci.*, 69(07)(2016): 911-920.
- [2] P. Aykov, "Computer modelling of a linear turbine for extracting energy from low-flowing waters", *Compt. rend. Acad. bulg. Sci.*, 67(08)(2014): 1159-1164.
- [3] C. Y. Lee, S.J. Lee, Y.M. Lo, Y.M. Liu, "Fuel cells dynamical analysis and modeling", *Int. J. Electrochem. Sci.*, (09) (2014): 272-281.
- [4] V. Duintam, A. Macchelli, S. Stramigioli, H. Bruyninckx, "Modeling and Control of Complex Physical Systems", Springer, 1st Ed., 2009.
- [5] S. Savov, I. Popchev, "Non-iterative improvement of trace bounds for the Lyapunov equation solution", *Compt. rend. Acad. bulg. Sci.*, 66(05)(2015): 733-738.
- [6] N. Obanov, N. Tezak, "Soft-switching converter for tram auxiliary power supply", 16th Conf. PEMC-Turkey, pp. 270-275, 2014.
- [7] B. K. Ose, "Power electronics and motion control - technology status and recent trends", *IEEE T. Ind. Appl.*, 29(05)(1993): 902-909.
- [8] S. Ildirmaz, H. Bodur, "A new ZVT snubber cell for PWM-CCM-PFC boost converters", 17th Conf. EPE'15-ECCE-Europe, pp. 590-600, 2015.
- [9] V. Udriashov, "A modified maximum likelihood method for estimation of mutual delay and power of noise signals by bistatic radiometer", *Compt. rend. Acad. bulg. Sci.*, 68(05)(2015): 631-640.